A 3D SEDIMENT TRANSPORT MODEL FOR COMBINED WAVE-CURRENT FLOWS

Peifeng Ma[1] and Ole Secher Madsen[2]

Accurate prediction of current velocity and bottom shear stress, which both can be significantly influenced by wind waves, is essential for sediment transport predictions in the coastal environment. Consequently wind-wave effects must be taken into account in a numerical sediment transport model for application in coastal waters. In the present study, elements of a large-scale 3D numerical coastal circulation and sediment transport model are developed to predict net, i.e. the wave-period-averaged, sediment transport rates. The sediment transport components considered are (i) bed-load transport; (ii) mean suspended load sediment transport within the wave boundary layer, which is obtained from an analytical solution; and (iii) suspended load sediment transport above the wave bottom boundary layer, which is obtained from a numerical model. In all model components wind wave effects are accounted for through simple analytical models. Thus, the roughness prescribed for the hydrodynamic part of the numerical coastal circulation model is the apparent roughness, i.e. the roughness experienced by a slowly varying current in the presence of waves. Similarly, the reference concentration specified for the sediment transport part of the numerical model is obtained from analytical solutions for suspended sediment concentrations within the combined wave-current bottom boundary layer. Stratification effects caused by suspended sediment are included in the large-scale numerical sediment transport model. Results of idealized tests suggest that wind wave effects can be pronounced, e.g. in some typical coastal scenarios sediment can only be mobilized when wind waves are present and accounted for. It is also shown that stratification can significantly affect suspended sediment transport rates of fine sediments.

Keywords: sediment transport; bottom boundary layer; wave-current interaction; sediment-induced stratification

1. INTRODUCTION

As illustrated in Figure 1, a typical coastal environment consists of wind waves, slowly varying currents, such as tide- and wind-driven flows, and sediment in the bottom and water column. Sediment can be moved as bed-load transport on the seabed or stirred up into the water column by bed shear stress and then transported by a current as suspended load transport. It is well-known that wind waves can intensify the near bottom turbulence significantly due to the limited thickness of the wave boundary layer. As a result, the bottom shear stress and turbulent mixing in the water column can be markedly enhanced by the presence of wind waves resulting in more sediment being mobilized and moved to upper layers of the water column where it is then made available for transport by currents. Consequently, wind wave effects must be included in numerical coastal circulation and sediment transport models. Since coastal circulation models cannot resolve the short time-scales governing the wave bottom boundary layer, the hydrodynamic as well as sediment transport processes within the combined wave-current bottom boundary layer must be calculated separately to produce physically realistic, slowly varying boundary conditions that are passed on to the numerical coastal circulation and sediment transport model.

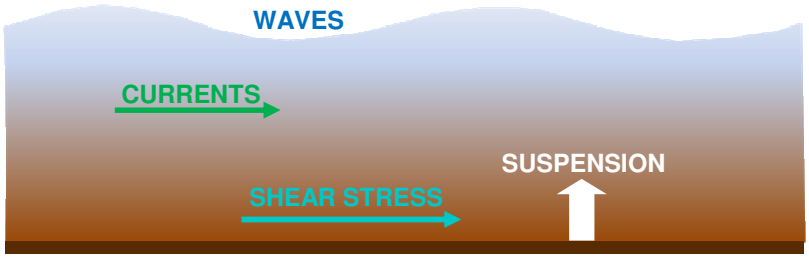

Figure 1 Illustration of a typical coastal environment

Many numerical sediment transport studies have been conducted in the past few decades (e.g. Li and Amos, 2001; Lesser et al., 2004; Warner et al., 2008). Wind wave effects have been taken into

[1] Singapore-MIT Alliance for Research and Technology, 1 CREATE way, #09-03 CREATE Tower, Singapore, 138602
[2] Parsons Laboratory, Massachusetts Institute of Technology, Room 48-216C, 15 Vassar Street, Cambridge, MA, 02139, USA

account in some models, e.g. some wave-associated coefficients are introduced by Lesser et al. (2004) to account for wave effects on sediment transport. Wave-current interaction models (e.g. Madsen, 1994) are introduced by Li and Amos (2001) and Warner et al. (2008) to predict combined wave-current shear stresses for sediment transport predictions. However, most numerical sediment transport models treat the wave boundary layer as a portion of numerical domain, regardless of the much different physics within the layer which usually cannot be resolved by coastal circulation models. Density changes caused by suspended sediment have been included in some sediment transport models (e.g. Lesser et al., 2004; Warner et al., 2008), but hardly any information has been reported on the importance of this sediment stratification effect.

The objective of the present study is to develop a three dimensional numerical sediment transport model for combined wave-current flows. A bottom boundary layer model is introduced to account for wind wave effects on current flow and sediment transport. The mean suspended sediment transport within the boundary layer is calculated separately and analytically. The sediment stratification effect is studied. The paper is organized as follows. A model description, including flow model, bottom boundary layer model and sediment transport model, is presented in Section 2. In Section 3, numerical experiments are conducted to test the model. Finally conclusions are provided in Section 4.

2. MODEL DESCRIPTION

In coastal waters, sediment is usually stirred up by the bed shear stress and then transported by a current. Bed shear stress determines the amount of sediment being mobilized and flow velocity determines how far the sediment can be transported. In the present model, a bottom boundary layer model is introduced to predict bed shear stress in combined wave-current flows, including the total and sediment transport shear stresses. A numerical coastal circulation model is used to compute eddy viscosity and velocity profiles for the slowly varying currents above the bottom boundary layer, for which wave effects are incorporated through the specification of an enhanced apparent bottom roughness, i.e. the roughness experienced by a current in the presence of wind waves. The bed-load transport rate and the reference concentration for suspended sediment concentration are computed from the so-called skin friction or sediment transport shear stress. The mean suspended load transport within the bottom boundary layer is solved analytically. The suspended load sediment transport rate above the bottom boundary layer is computed by a numerical sediment transport model that solves the unsteady, i.e. slowly varying, advection-diffusion equation to obtain the suspended sediment concentration corresponding to a specified reference concentration predicted by the analytical bottom boundary layer model that includes the effects of wind waves.

The present model is formulated in a terrain following coordinate system (x, y, σ) with x and y indicating the two directions in the horizontal plane and σ representing the scaled vertical direction. The velocities in the three directions are denoted by (u, v, w). The still water depth is h and surface elevation is denoted by η. The water density and molecular viscosity are taken to be ρ = 1,025kg/m^3 and ν = 1.3x10^{-6}m^2/s, respectively. To be realistic, we assume the presence of random wind waves which have a root mean square (rms) wave height H_r and a representative wave period T_r or angular frequency $\omega_r = 2\pi / T_r$ and assumed described by linear wave theory. Non-cohesive sediment with median diameter d and density ρ_s = 2,650kg/m^3 is considered in the present study.

2.1 Hydrodynamic Model

The Princeton Ocean Model (POM), Blumberg and Mellor (1987), is used to predict 3D flow velocities (u, v, w) in the x, y and σ directions, respectively. POM is a primitive equation ocean model based on hydrostatic and Bousinesq assumptions, in which the turbulence closure scheme of Mellor and Yamada (1982), hereafter referred to as MY, is incorporated to estimate eddy viscosity K_M and eddy diffusivity for heat, K_H. In the present study, we assume the suspended sediment diffuses in the same way as the heat and therefore take the sediment eddy diffusivity $K_S = K_H$. As pointed out by Warner et al. (2005), the MY scheme predicts a substantially smaller eddy viscosity than analytical solutions and other turbulence closure schemes. This under-prediction may have significant influence on suspended sediment concentrations causing it to decay too rapidly with distance from the bed. To avoid the under-prediction, the wall proximity function with open channel correction proposed by Blumberg et al. (1992) is used to replace the original wall function in the MY scheme. Since POM cannot resolve the small scale wave motion, only net or wave-period averaged quantities are computed in the present study, e.g. the net bed-load transport rate and mean concentrations.

2.2 Bottom Boundary Layer Model

A wave-current interaction model (Grant and Madsen, 1979; Madsen, 1994; Humbyrd and Madsen, 2010) is incorporated into POM to account for wind wave effects. The model is based on a bilinear time-invariant eddy viscosity model that is proportional to the combined maximum wave-current shear velocity u_{*m} within and to the enhanced current shear velocity u_{*c} above the bottom boundary layer, i.e.

$$K_M(z) = \begin{cases} \kappa u_{*m} z, & z \le \delta_{cw} \\ \kappa u_{*c} z, & z \ge \delta_{cw} \end{cases} \tag{1}$$

The model is able to predict the physical, i.e. movable, bottom roughness k_n, the apparent bottom roughness, i.e. the enhanced bottom roughness experienced by a current in the presence of waves, k_{na}, the wave boundary layer thickness δ_{cw}, the total current and wave shear velocities, u_{*c} and u_{*wm}, and the current and wave skin friction, or sediment transport, shear velocities u_{*cs} and u_{*wms}.

The information required to implement the wave-current interaction model include: water depth h; rms wave height H_r and period T_r or angular frequency ω_r; current bottom shear velocity u_{*c} or a reference current velocity u_r at $z = z_r$; and sediment diameter d. The solution procedure for the wave-current interaction can be divided into three steps.

2.2.1 Prediction of physical bottom roughness k_n based on wave and sediment specification

It is assumed that wind waves dominate fluid-sediment interaction and therefore determine the bed condition, i.e. flat without or with sediment motion or rippled, so that the physical roughness can be predicted solely from wave information. To do this, the maximum wave bottom orbital velocity U_{bm} or the excursion amplitude $A_{bm} = U_{bm} / \omega_r$ is computed from rms wave height, period and water depth. Then the skin friction Shields Parameter $\psi_d^{'}$ is obtained from

$$\psi_d^{'} = \tau_{wm}^{'} / \left[\rho(s-1)gd\right] = 0.5 f_w^{'} U_{bm}^2 / \left[(s-1)gd\right] \tag{2}$$

where $g = 9.81\text{m}^2/\text{s}$ is the acceleration due to gravity and $s = \rho_s / \rho = 2.59$ is the relative density of sediment. The wave skin friction factor $f_w^{'}$ is computed based on a bottom roughness equal to the median sediment diameter, i.e.

$$f_w^{'} = \begin{cases} \exp\left[7.02X^{-0.078} - 8.82\right], & X = A_{bm}/d < 10^2 \\ \exp\left[5.61X^{-0.109} - 7.30\right], & X = A_{bm}/d \ge 10^2 \end{cases} \tag{3}$$

There will be no sediment motion if the skin friction Shields Parameter $\psi_d^{'}$ given by (2) is smaller than the critical value, ψ_{cr}, which can be estimated by the formula proposed by Herrmann and Madsen (2007)

$$\psi_{cr} = 0.095 S_*^{-2/3} + 0.056\left[1 - \exp\left(-S_*^{3/4} / 20\right)\right] \tag{4}$$

where $S_* = d\sqrt{(s-1)gd} / 4\nu$. The bed will be flat with no transport if $\psi_d^{'} < \psi_{cr}$, rippled if $\psi_{cr} \le \psi_d^{'} \le 0.35$ and in sheet flow condition if $\psi_d^{'} > 0.35$. The threshold Shields Parameter for sheet flow condition is taken to be 0.35, rather than the usual value of 0.7, because the Shields Parameter computed using the significant wave orbital velocity, $\psi_s^{'} = 2\psi_d^{'}$, has been found to describe onset of sheet flow for random waves. The threshold Shields Parameter for initiation of motion is still taken as ψ_{cr} in order to be consistent with the critical value used in the calculation of bed-load transport rate and reference concentration for sediment suspension in combined wave-current flows.

The physical roughness for different bed conditions can therefore be computed from

$$k_n = \begin{cases} d, & \psi_d^{'} < \psi_{cr} \text{ (no transport)} \\ k_n\left(d, A_{bm}/k_n\right), & \psi_{cr} \le \psi_d^{'} \le 0.35 \text{(rippled bed)} \\ \max(d, A_n d), & \psi_d^{'} > 0.35 \text{ (sheet flow)} \end{cases} \tag{5}$$

where A_n is a function of $\psi_d^{'}$ suggested to be $15\psi_d^{'}$ by Madsen (2002) based on very limited data.

For rippled bed conditions, the physical roughness in (5) can be calculated iteratively through the empirical relationship for the energy dissipation factor established by Humbyrd and Madsen (2010)

$$f_e = 0.14 S_*^{0.25} \exp\left(-4.94\psi_d^{'}\right) \tag{6a}$$

This energy dissipation factor is a function of bottom roughness

$$f_e = f_w \cos\left\{(\pi/60)\left[11 - 2\log_{10}\left(A_{bm}/k_n\right)\right]\right\} \tag{6b}$$

where f_w is computed from (3) with $X = A_{bm}/k_n$. Therefore, the energy dissipation factor f_e can be calculated by (6a) based on the skin friction Shields Parameter obtained from (2). Having f_e, the physical roughness can be computed iteratively from (6b).

2.2.2 Prediction of total shear velocities, boundary layer thickness and apparent roughness

With the physical bottom roughness k_n obtained as outlined in Section 2.2.1, and the current shear velocity u_{*c}, a wave-current interaction analysis can be performed to yield the maximum wave shear velocity, u_{*wm}. The general procedure is

$$C_\mu = \left(1 + 2\left|\cos\phi_{cw}\right|\mu + \mu^2\right)^{1/2} \quad \text{with } \mu = u_{*c}^2 / u_{*wm}^2 \tag{7a}$$

$$f_{cw} = \begin{cases} C_\mu \exp\left[7.02 X_\mu^{-0.078} - 8.82\right], & X_\mu = C_\mu A_{bm}/k_n < 10^2 \\ C_\mu \exp\left[5.61 X_\mu^{-0.109} - 7.30\right], & X_\mu = C_\mu A_{bm}/k_n \geq 10^2 \end{cases} \tag{7b}$$

$$u_{*wm} = \sqrt{f_{cw}/2}\, U_{bm} \tag{7c}$$

where $\phi_{cw} = \phi_c - \phi_w$ is the angle between currents and waves, with ϕ_c and ϕ_w denoting the current and wave directions with respect to the x axis. In this wave-current interaction procedure, the current shear stress or shear velocity u_{*c} is kept unchanged since it would be slowly varying. But this does not mean the current shear stress is fixed for the entire simulation, since it varies slowly with time as predicted by the numerical circulation model and/or slowly changing wind wave conditions. Hence, the bottom boundary layer model and the flow model are fully coupled.

Once the iteration procedure in (7a-c) converges, we can obtain u_{*c} and u_{*wm} and the combined maximum shear velocity $u_{*m} = \sqrt{C_\mu}\, u_{*wm}$, from which we can calculate the bottom boundary layer thickness

$$\delta_{cw} = P A_\mu \kappa u_{*m} / \omega_r \tag{8a}$$

where

$$A_\mu = \exp\left[2.96\left(C_\mu A_{bm}/k_n\right)^{-0.071} - 1.45\right] \tag{8b}$$

$$P = \frac{1}{16.3}\left(\sqrt{C_\mu/\mu}\right)^{\sqrt{C_\mu}/\left(\sqrt{C_\mu}-\sqrt{\mu}\right)} \tag{8c}$$

The current velocity within and above the boundary layer can now be computed from

$$u_c(z) = \begin{cases} u_{*c}^2/\kappa u_{*m} \cdot \ln\left(30z/k_n\right), & z \leq \delta_{cw} \\ u_{*c}/\kappa \cdot \ln\left(30z/k_{na}\right), & z \geq \delta_{cw} \end{cases} \tag{9}$$

where the apparent roughness, k_{na}, is obtained by matching the velocity at $z = \delta_{cw}$

$$k_{na} = 30\delta_{cw}\left(30\delta_{cw}/k_n\right)^{-u_{*c}/u_{*m}} \tag{10}$$

The apparent roughness is the roughness experienced by the current in the presence of wind waves, which is used to compute the quadratic bottom friction factor

$$C_D = \kappa^2 / \left[\ln\left(30 z_1 / k_{na}\right)\right]^2 \tag{11}$$

where z_1 is the first interior velocity grid level above the bottom in POM simulations . A logarithmic velocity distribution near the bottom is assumed to obtain (11). Through this bottom friction factor, C_D, the numerical circulation model captures the enhancement of bottom resistance induced by wind waves. The apparent roughness is the only parameter passing from the bottom boundary layer model to the flow model, which in turn will provide an updated current shear stress to the bottom boundary layer model. The current bottom shear stress τ_{bc} in POM is computed from the friction factor and the horizontal velocity U_1 at the level $z = z_1$

$$\tau_{bc} = \rho C_D U_1^2 \tag{12}$$

2.2.3 Prediction of sediment transport shear stress

To compute sediment transport rates, we need to evaluate the shear stresses or shear velocities responsible for moving and entraining sediment. For sheet flow conditions, the shear stresses obtained as outlined above are the sediment transport shear stresses. For rippled bed conditions, the total shear stresses obtained in the preceding section consist of skin friction and form drag, and of these only the skin friction shear stress is responsible for sediment motion. Thus, when the bed is rippled, the skin friction shear stress needs to be separated from the total shear stress. To do this, another wave-current interaction analysis is performed based on a reference current velocity and a skin friction roughness.

For rippled bed conditions, a reasonable skin friction roughness should be related to the flow intensity rather than a constant multiple of the grain size. In order to make a smooth transition from rippled bed to sheet flow conditions, we adopt the roughness for sheet flow condition in (5) to calculate skin friction bottom roughness, i.e. we take

$$k_{ns} = \max(d, 15\psi_d' d) \tag{13}$$

Unfortunately, no experimental data are available to support a specific choice of the reference level for the reference current velocity to be used in the computation of the sediment transport shear stresses for combined wave-current flows. Thus we choose, somewhat arbitrarily but physically and computationally pleasing, the upper boundary of the wave bottom boundary layer as the reference level at which the reference current velocity is specified, i.e. we have from (9)

$$u_r = \left(u_{*c} / \kappa\right) \ln 30\delta_{cw} / k_{na} \quad \text{at} \quad z_r = \delta_{cw} \tag{14}$$

Hence the sediment transport shear velocities u_{*cs} and u_{*wms} can be computed from the following iterative procedure

$$C_{\mu s} = \left(1 + 2\left|\cos\phi_{cw}\right|\mu_s + \mu_s^2\right)^{1/2} \quad \text{with } \mu_s = u_{*cs}^2 / u_{*wms}^2 \tag{15a}$$

$$f_{cws} = \begin{cases} C_{\mu s} \exp\left[7.02 X_s^{-0.078} - 8.82\right], & X_s = C_{\mu s} A_{bm} / k_{ns} < 10^2 \\ C_{\mu s} \exp\left[5.61 X_s^{-0.109} - 7.30\right], & X_s = C_{\mu s} A_{bm} / k_{ns} \geq 10^2 \end{cases} \tag{15b}$$

$$u_{*wms}^2 = 0.5 f_{cws} U_{bm}^2 \tag{15c}$$

$$u_{*ms} = \sqrt{C_{\mu s}}\, u_{*wms} \tag{15d}$$

$$u_{*cs} = u_{*ms} \frac{\ln(z_r / \delta_{cws})}{\ln(\delta_{cws} / z_{0s})} \left[-\frac{1}{2} + \sqrt{\frac{1}{4} + \frac{\kappa u_r \ln(\delta_{cws} / z_{0s})}{u_{*ms} \ln(z_r / \delta_{cws})^2}} \right] \tag{15e}$$

where $z_{0s} = k_{ns} / 30$ and the thickness δ_{cws} is computed in the same way as δ_{cw} in (8a-c) but with the skin friction parameters $k_{ns}, \mu_s, C_{\mu s}$ and u_{*ms}. After the iteration procedure in (15a-e) converges, we can obtain the sediment transport shear stresses for the current, $\tau_{cs} = \rho u_{*cs}^2$, and for the waves, $\tau_{wms} = \rho u_{*wms}^2$. The total sediment transport shear stress can then be written as

$$\begin{aligned}\vec{\tau}_{bs}(t) &= \left[\tau_{bsx}(t),\quad \tau_{bsy}(t)\right] \\ &= \left[\tau_{wms}\cos\omega_r t\cos\phi_w + \tau_{cs}\cos\phi_c, \tau_{wms}\cos\omega_r t\sin\phi_w + \tau_{cs}\sin\phi_c\right]\end{aligned} \tag{16}$$

2.3 Sediment Transport Model

Instantaneous sediment transport rates are averaged over a wind wave period to yield mean or net sediment transport rates. Three categories of sediment transport are considered: (i) Net bed load transport, $\bar{\boldsymbol{q}}_{\boldsymbol{B}}$, which takes place below the reference level for mean concentration specification for the suspended load, $z = 7d$; (ii) Mean suspended load transport within the wave boundary layer, $7d < z < \delta_{cw}$, $\bar{\boldsymbol{q}}_{\boldsymbol{S1}}$, which is obtained from analytical solutions for current velocity and mean sediment concentration within the wave boundary layer, since POM does not resolve wave boundary layer scales; and (iii) Mean suspended load transport above the wave boundary layer, $z > \delta_{cw}$, $\bar{\boldsymbol{q}}_{\boldsymbol{S2}}$, which is obtained by solving an advection-diffusion equation for the mean sediment concentration and the current velocity using POM.

The instantaneous bed-load mass transport rate is computed by the model proposed by Madsen (1991).

$$\vec{q}_B(t) = Max\left\{\left|\vec{\tau}_{bs}(t) - \tau_{cr,\beta}\right|, 0\right\}\cdot\frac{8\rho_s}{\rho^{1.5}(s-1)g}\cdot\frac{\left(\sqrt{\left|\vec{\tau}_{bs}\right|} - \alpha_\beta\sqrt{\tau_{cr,\beta}}\right)}{\tan\varphi_m - \tan\beta}\cdot\frac{\vec{\tau}_{bs}}{\left|\vec{\tau}_{bs}\right|} \tag{17}$$

where β is the bottom slope in the direction of the instantaneous sediment transport shear stress and considered positive when sloping up in the shear stress direction. In large scale coastal simulations, the bed slope is usually very small, i.e. $\tan\beta \approx \sin\beta \approx \beta << 1$. The critical shear stress with slope effect is given by $\tau_{cr,\beta} = \tau_{cr}\left(1 + \tan\beta / \tan\varphi_s\right)$ with $\tau_{cr} = \psi_{cr}\left[\rho(s-1)gd\right]$ and ψ_{cr} computed by (4). φ_s and φ_m are static and dynamic friction angles for sediment which have values of 30^o and 50^o, respectively. Thus, the parameter $\alpha_\beta = \sqrt{\left(\tan\varphi_m + \tan\beta\right)/\left(\tan\varphi_s + \tan\beta\right)} \approx 0.7$.

The net bed-load transport rate can be computed by averaging (17) over a wave period as

$$\bar{\boldsymbol{q}}_{\boldsymbol{B}} = \frac{1}{T}\int_0^T \vec{q}_B(t)\,dt \tag{18}$$

The instantaneous bed-load transport rate for a pure sinusoidal wave condition is $\vec{q}_B(t) \propto \sqrt{\left|\tau_{wms}\cos\omega_r t\right|}\cdot\tau_{wms}\cos\omega_r t$, which obviously leads to a period-averaged bed-load transport of zero. Thus, wind waves can only give rise to a non-zero net bed-load transport when they are acting together with a current and/or on a sloping bottom. For example, if we assume wave shear stress to be dominant and the bed slope to be small, the net bed-load transport was shown by Madsen (2002) to be approximately given by $\bar{\boldsymbol{q}}_{\boldsymbol{B}} \propto 9u_{*wms}\left(u_{*cs}^2 - u_{*wms}^2\tan\beta / 2\tan\varphi_m\right)$.

To predict suspended load transport rate above the bed-load transport layer, i.e. $z > 7d$, a reference concentration at $z = 7d$, related to the excess sediment transport shear stress, was introduced by Madsen (2002)

$$C_R(t) = 0.0022\rho_s c_0\max\left[\left(\left|\vec{\tau}_{bs}(t)\right| / \tau_{cr,\beta} - 1\right), 0\right] \quad \text{at } z = 7d \tag{19}$$

where $c_0 = 0.65$ is the volume concentration of sediment in the bed. Again, only the mean reference concentration is considered here, which is

$$\bar{C}_R = \frac{1}{T}\int_0^T C_R(t)dt \tag{20}$$

It can be shown that, unlike the net bed-load transport, linear wind waves alone can produce a significant mean reference concentration, e.g. the mean concentration for pure wave conditions can be expressed by $\bar{C}_R = 0.0044/\pi\rho_s c_0\left(\tau_{wms}/\tau_{cr} - 1\right)$ which obviously does not vanish. Therefore, wave-induced bottom shear stress can play a very important role in predicting suspended load transport and

should not be neglected, especially for wave dominated conditions which are common in most coastal waters.

Since the large scale numerical model does not resolve wave bottom boundary layer scales, the mean concentration in this layer is computed analytically based on an eddy diffusivity K_S which is assumed identical to the eddy viscosity, K_M, given by (1). To obtain the analytical concentration solution, we assume the time scale of vertical diffusion in the boundary layer is much smaller than the scale of the slow current flow changes so that equilibrium can be assumed. This assumption should be reasonable, since the wave boundary layer is thin and the turbulent mixing is very strong. For equilibrium, the vertical diffusion and the sediment settling effects are balanced to yield an analytical concentration solution within the wave boundary layer

$$\bar{C}(z) = \bar{C}_R \left(z / 7d \right)^{-w_f / \kappa u_{*m}} \tag{21}$$

where w_f is the sediment fall velocity. It is calculated from the formula proposed by Jiménez and Madsen (2003)

$$w_f = \sqrt{(s-1) g d_n} \,/ \left(0.95 + 5.1 / S_{*n}\right) \tag{22}$$

where $d_n \approx d / 0.9$ and $S_{*n} = d_n \sqrt{(s-1) g d_n} / 4\nu$.

Therefore the net suspended load transport rate in the wave bottom boundary layer is

$$\bar{\boldsymbol{q}}_{\boldsymbol{SI}} = \int_{7d}^{\delta_{cw}} \vec{u}_c \bar{C} dz \tag{23}$$

where the current velocity vector $\vec{u}_c(z)$ is given by (9). This integration of (23) can be performed analytically (e.g. Madsen, 2002) or numerically by discretizing the boundary layer into a large number of layers. In the present study, the latter method is adopted.

The hydrodynamic and sediment transport processes above the boundary layer are far more complex than their counterparts within the bottom boundary layer and are solved numerically in the present study. The slowly varying current velocity is computed from the numerical circulation model, POM, whereas the mass concentration $C(z)$ is obtained by numerically solving the advection-diffusion equation for suspended sediment,

$$\begin{aligned} &\frac{\partial DC}{\partial t} + \frac{\partial}{\partial x}(DuC) + \frac{\partial}{\partial y}(DvC) + \frac{\partial}{\partial \sigma}\left[(w - w_f)C\right] = \\ &\qquad \frac{\partial}{\partial \sigma}\left(\frac{K_S}{D}\frac{\partial C}{\partial \sigma}\right) + \frac{\partial}{\partial x}(A_H D \frac{\partial C}{\partial x}) + \frac{\partial}{\partial y}(A_H D \frac{\partial C}{\partial y}) \end{aligned} \tag{24}$$

where $D = h + \eta$ is the total water depth with η the free surface elevation predicted by POM, A_H is the horizontal eddy diffusivity which is assumed the same as the horizontal eddy viscosity and predicted by POM, and the vertical diffusivity for sediment, K_S, is assumed identical to the heat diffusivity predicted by MY turbulence closure scheme in POM.

Boundary conditions need to be specified in order to solve (24). At land boundaries, a no flux condition is applied, i.e. $\partial C / \partial n = 0$ with n denoting the outward normal direction at the boundary. At open boundaries, concentration is specified for inflow condition, i.e. $C = C_{in}$ if $u_n < 0$ with u_n the flow velocity in the outward normal direction, n, and an advection condition is applied for outflow, i.e. $\partial C / \partial t + u_n \partial C / \partial n = 0$ if $u_n > 0$. At the free surface, zero net sediment flux is assured by setting $K_S \partial C / \partial \sigma + D w_f C = 0$ at $z = h + \eta$, whereas a sediment concentration, the reference concentration, is specified as $C = C_b$ at bottom.

To obtain the reference concentration, C_b, we first compute the mean concentration at the outer edge of the wave boundary layer, i.e. at $z = \delta_{cw}$, from the analytical wave boundary layer solution, (21),

$$C_a = \bar{C}(z = \delta_{cw}) = \bar{C}_R \cdot \left(\delta_{cw} / 7d\right)^{-w_f / \kappa u_{*m}} \tag{25}$$

Physically, the bottom level in POM simulations is defined at the outer edge of the wave boundary layer, i.e. $z = \delta_{cw}$. However, due to the staggered grid system used in POM, the bottom level for

concentration is not at $z = \delta_{cw}$ but a half grid spacing above it, i.e. at $z = z_b = \delta_{cw} + \Delta z_b / 2$ with Δz_b the spacing for the interior grid cell immediately above the bottom. Assuming equilibrium conditions to apply within the bottom half of the first grid, the concentration C_b can be obtained analytically based on the reference concentration C_a at $z = \delta_{cw}$ and the linear eddy diffusivity above the boundary layer given by (1). In this manner, the reference concentration for the large scale numerical sediment transport model clearly accounts for wind wave effects and it becomes

$$C_b = C_a \left(1 + \Delta z_b / 2\delta_{cw}\right)^{-w_f / \kappa u_{*c}} \text{ at } z = z_b \tag{26}$$

The eddy diffusivity predicted by POM approaches zero at the bottom level which is actually at the outer edge of the wave boundary layer where the eddy diffusivity according to the wave boundary layer model should be $\kappa u_{*c} \delta_{cw}$. This relatively small eddy diffusivity may produce a large difference in sediment concentration, since suspended sediment concentration is very sensitive to the diffusivity near the bottom. For example, if we assume a typical condition with $w_f = 1cm/s$, $u_{*c} = 2.5cm/s$, $\delta_{cw} = 5cm$, $\Delta z_b = 10cm$ and $C_a = 1kg/m^3$, we obtain $C_b = 0.5kg/m^3$ from (26), and the concentration at the upper boundary of the first grid cell, $z = \delta_{cw} + \Delta z_b$ is roughly 0.33kg/m^3. If directly using the eddy diffusivity predicted by POM, the concentration at $z = \delta_{cw} + \Delta z_b$ predicted by the present model can be estimated analytically to be $0.25kg/m^3$. This underestimates the concentration by about 24%. To avoid this under-predictions and be more physically consistent, we add the constant eddy diffusivity, $\kappa u_{*c} \delta_{cw}$, to the POM predicted eddy diffusivity K_{SPOM} over the entire water depth

$$K_S = K_{SPOM} + \kappa u_{*c} \delta_{cw} \tag{27}$$

This adjustment may lead to some minor error in eddy diffusivity near the surface as it does not approach zero. However, this error should have very little influence on the predicted sediment concentration as it is usually quite small near the free surface.

Having the flow velocity and the concentration, the suspended load transport rate above the wave boundary layer is computed by

$$\vec{q}_{S2} = \int_{\delta_{cw}}^{h+\eta} \vec{u} C dz \tag{28}$$

Suspended sediment will change the water-sediment mixture density and therefore produce stratification, which in turn will affect the predictions of flow velocity and sediment concentration. The density of the water-sediment mixture can be computed from

$$\rho_{mix} = \rho + C(z)(1 - 1/s) \tag{29}$$

A stable stratification, which would generally be the case for sediment suspended in the water column since the concentration and therefore the mixture density would decrease with distance above the bottom, suppresses the turbulence and therefore weakens the turbulent mixing. This would result in an increase in velocity and a reduction in sediment concentration. In contrast, an unstable stratification intensifies the flow turbulence and therefore results in more sediment transport. Due to the sediment settling effect, positive stratification should be more common. Unstable stratification may, however, occur in rapidly varying flows when the near-bed concentration, which responds nearly instantaneously to the reference concentration, decreases so rapidly that high sediment concentrations in upper layers have insufficient time to settle out of suspension.

3. MODEL TESTS

In this section, a few idealized tests are performed to examine the model's ability to predict wind wave effects and sediment transport in combined wave-current flows. The computational domain is an open channel of 100km length, 10km width and 10m depth. In the numerical simulations, uniform horizontal grid cells of Δx = Δy = 2km and 40 non-uniform sigma layers with finer spacing near the bed are used. The external and internal time steps are 6sec and 120sec, respectively.

In the tests, Coriolis force is neglected. A steady open channel flow is considered which is driven by a prescribed constant volume discharge at both open boundaries, equivalent to applying a depth-

averaged velocity $U = 0.5/(1+\eta/h)$ m/s at the boundaries. This leads to U = 0.5m/s at the center of the domain where the surface elevation $\eta = 0$ after a steady state is established. The flow is uniform in the cross-channel direction. A random wind wave condition with a rms height of H_r = 1m and a representative period of T_r = 8sec is specified. The waves are assumed to propagate in the same direction as the current flow, i.e. this is a co-directional combined wave-current flow case. Uniform sediment with a median grain size of d = 0.1mm or 0.2mm is assumed. This corresponds to a critical shear stress of $\tau_{cr} = 0.19N/m^2$ or $0.20N/m^2$ or a critical shear velocity of $u_{*cr} = 1.36cm/s$ or $1.40cm/s$ as computed from (4) and a fall velocity of $w_f = 0.72cm/s$ or $2.2cm/s$ from (22). For the inflow boundary condition, the sediment concentration is assumed zero. This creates a transition region near the upstream boundary. The length of this transition region can be estimated approximately from $L = Uh^2/K_S \sim 0.5\times10^2/0.01 = 5km$. Evidently, this is a very short distance compared to the domain length of 100km, most of which will therefore be unaffected by transition effects.

The simulations are run for 3 days. To avoid simulation crash, the forcing is imposed gradually with a linear ramp up during the first 12hours. The results show that steady state is established within a few hours after the ramp up period. All the results shown in this Section are obtained at the center of the domain where the surface elevation is close to zero at a time corresponding to the end of the simulation, t = 72 hours.

For the 0.1mm sediment, three simulations are performed: (1) Pure current case; (2) Combined wave-current case without stratification; (3) Combined wave-current case with stratification. For the 0.2mm sediment, only simulations (2) and (3) are performed. Some predicted parameters for simulations (2) and (3) are listed in Table 1, including physical bottom roughness, apparent roughness, boundary layer thickness, wave and current shear velocities and reference concentrations. Sediment transport rates are listed in Table 2 for the different simulations.

3.1 Effects of Wind Waves

The vertical profiles of eddy viscosity and horizontal velocity from simulations (1) and (2) for 0.1mm sediment are shown in Figure 2. For the pure current simulation, the physical roughness is chosen to be the larger one of the sediment diameter d and $3.3\nu/u_{*c}$, i.e. the simulation starts with $k_n = d$ by assuming a rough turbulent flow, then checks and switches to smooth turbulent flow with $k_n = 3.3\nu/u_{*c}$ if $d < 3.3\nu/u_{*c}$. The flow model predicts a bottom shear velocity of 1.5cm/s, indicating a smooth turbulent flow condition and therefore the roughness is $k_n = 3.3\nu/u_{*c}$ = 0.28mm. When wind waves are present, a rippled bed is obtained, leading to a much larger physical roughness of k_n = 1.66cm and an apparent roughness of k_{na} =11.1cm (non-stratified case in Table 1) and a bottom shear velocity of 2.72cm/s. As a result, the maximum eddy viscosity (seen in Figure 2a) almost doubles from $0.01m^2/s$ to $0.02m^2/s$ due to the presence of wind waves. The current velocity profiles in Figure 2b show that the presence of wind waves leads to a lower current velocity near the bed due to the larger flow resistance. The velocity at the first interior grid point is decreased from about 0.3m/s for the pure current condition to 0.15m/s in the presence of wind waves.

Table 1. Parameters predicted by the model for different sediment in stratified and non-stratified flows.

Diameter	0.1mm		0.2mm	
Stratified Parameters	No	Yes	No	Yes
k_n (cm)	1.66	1.66	12.3	12.3
k_{na} (cm)	11.1	14.1	51.8	53.1
δ_{cw} (cm)	1.82	1.91	4.31	4.35
u_{*c} (cm/s)	2.72	2.24	3.43	3.34
u_{*cs} (cm/s)	1.24	1.00	0.88	0.85
u_{*wm} (cm/s)	5.30	5.20	8.14	8.12
u_{*wms} (cm/s)	2.82	2.76	2.80	2.80
$\bar{C}_R$ (kg/m^3)	7.23	6.75	6.39	6.34
C_a (kg/m^3)	2.72	2.38	0.75	0.73

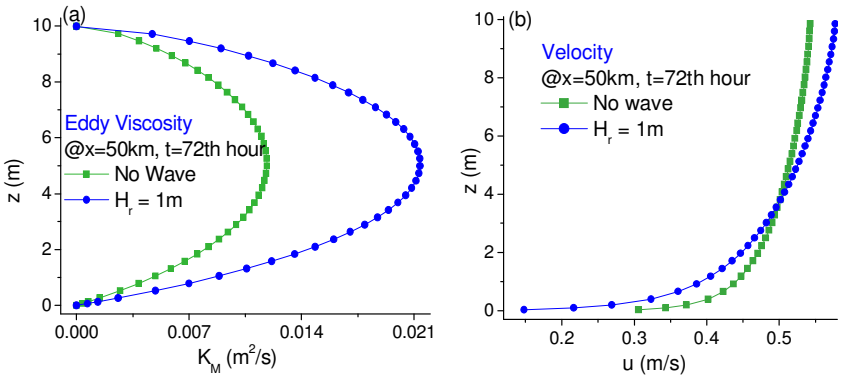

Figure 2. Predicted vertical profiles of (a) eddy viscosity and (b) current velocity for pure current and combined wave-current cases at the center of domain. Sediment size is 0.1mm.

Due to the flat bed condition, the sediment transport shear velocity for the pure current condition is equal to the total value of 1.5cm/s, which is very close to the critical shear velocity of 1.36cm/s for the 0.1mm sediment. This means that there is essentially no sediment transport for the pure current condition. In the presence of wind waves the sediment transport shear velocities are calculated to be 1.24 cm/s and 2.82cm/s for current and waves, respectively, and are based on a reference current velocity of u_r = 11.1cm/s at z_r = 1.82cm and a skin friction roughness of k_{ns} = 0.45mm. Hence, the sediment transport shear stress in this co-directional flow case is $\vec{\tau}_{bs}(t) = (0.8\cos\omega t + 0.15, 0)\, N/m^2$. This gives a maximum instantaneous value of 0.95 N/m^2, which is much larger than the critical shear stress of 0.19N/m^2. The rather dramatic effect of the presence of wind waves is seen in the reference concentrations, 7.23kg/m^3 and 2.72kg/m^3 (Table 1), at the lower and upper boundaries of the wave boundary layer. As shown in Table 2, the predicted transport rates are 0.01kg/m/s, 0.0051kg/m/s and 0.5kg/m/s for the net bed-load transport, the mean suspended load transport within and above the boundary layer, respectively. It can be seen that suspended load transport in the water column is dominant as it is about 30 times the combined bed-and suspended load transport rate within the wave boundary layer. This is mainly caused by the small fall velocity of the fine sediment and strong turbulent mixing enhanced by wind waves. Due to the thin boundary layer and fine sediment, the mean suspended load transport rate within the boundary layer is much smaller than that in the overlying water column, but it is still comparable to the net bed-load transport rate.

Table 2. Transport rates (kg/m/s) of net bed-load, suspended load within and above the w.b.b.l. for two types of sediment. The total transport rate q_T is $\bar{q}_T = \bar{q}_B + \bar{q}_{S1} + \bar{q}_{S2}$.

	$\bar{q}_B$		$\bar{q}_{S1}$		$\bar{q}_{S2}$		$\bar{q}_T$	
Stratified Diameter *d*	No	Yes	No	Yes	No	Yes	No	Yes
0.1mm	1.0×10^{-2}	7.3×10^{-3}	5.1×10^{-3}	3.5×10^{-3}	5.0×10^{-1}	1.2×10^{-1}	5.2×10^{-1}	1.3×10^{-1}
0.2mm	6.2×10^{-3}	5.9×10^{-3}	3.1×10^{-3}	2.9×10^{-3}	1.6×10^{-2}	1.3×10^{-2}	2.5×10^{-2}	2.2×10^{-2}

3.2 Effects of Sediment-Induced Self-stratification for 0.1mm Sediments

Sediment stratification effects are accounted for in the present study by considering the stratification effects associated with the varying density of the water-sediment mixture as expressed in (29). The routine available in POM to account for stratification due to heat and/or salinity gradient is used to account for sediment stratification effects. In general, the stratification effect is incorporated by relating a turbulent kinetic energy (TKE) production to the vertical density gradient. This leads to an enhanced turbulence intensity by a positive vertical density gradient and vice versa. In this steady flow case, the concentration decreases all the way from the bed to surface, leading to stably stratified conditions which mean that the turbulence intensity will be reduced and therefore turbulent mixing will be weakened. This is confirmed by the decreased current shear velocity of 2.24cm/s predicted by POM and listed in Table 1 for 0.1mm sediment when stratification is accounted for compared to 2.72cm/s for

the non-stratified case. As a result, the current velocity within the boundary layer (seen in Figure 3a) shows quite a significant reduction, e.g. the velocity at the outer edge of the boundary layer is decreased from 11cm/s to 8cm/s. It should be recalled that stratification effects within the wave boundary layer are not accounted for, and this is the reason why the wave shear velocity, as seen in Table 1, hardly changes (it goes from 5.3cm/s to 5.2cm/s). The reduced current shear velocity, in addition to the reduced mixing associated with stable stratification, makes the eddy diffusivity above the wave boundary layer decrease substantially as shown in Figure 4a, reducing the maximum value from about 0.027m^2/s to 0.015m^2/s.

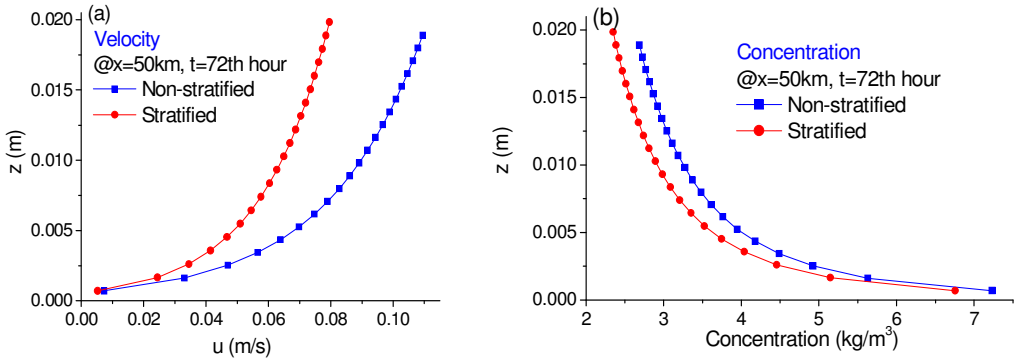

Figure 3 Analytical solutions of vertical profiles of (a) current velocity and (b) sediment concentration within the wave boundary layer at the center of domain. Sediment size is 0.1mm.

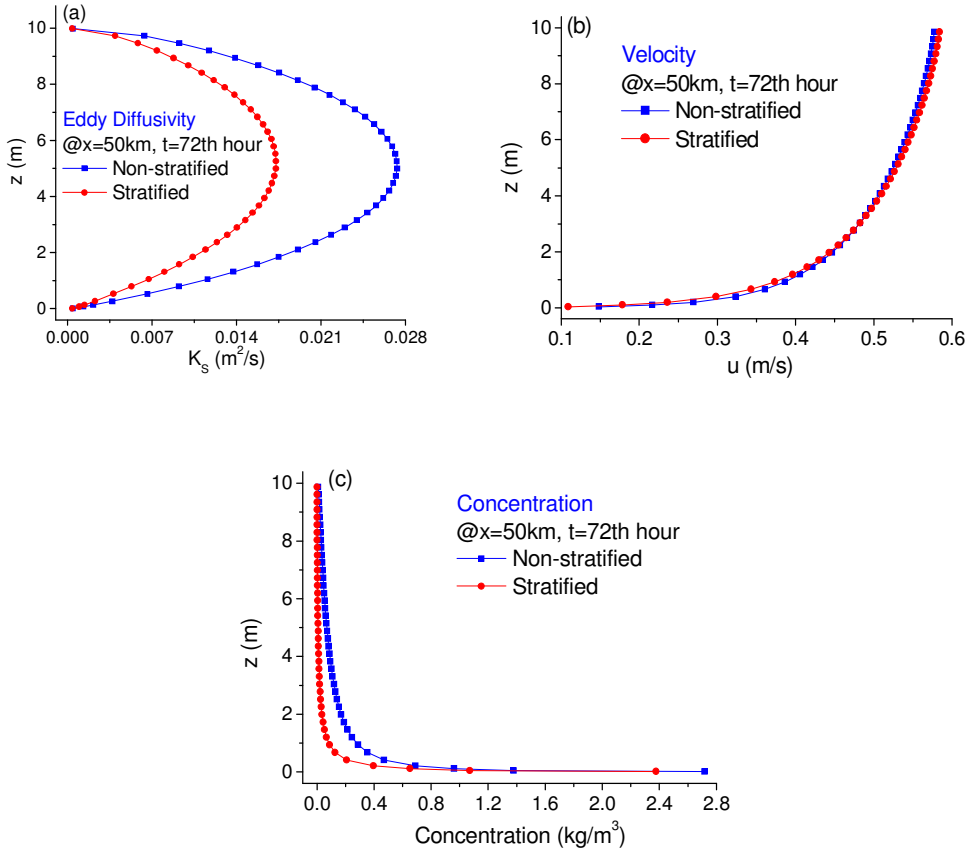

Figure 4 Predicted vertical profiles of (a) eddy viscosity; (b) Velocity; (c) Concentration above the wave boundary layer at the center of domain. Sediment size is 0.1mm.

Due to the reduced current shear velocity, the velocity gradient near the bottom decreases, but this tendency is counteracted by the reduced mixing due to stable stratification which would tend to increase the velocity gradient. The combined effect of these processes is a decrease of velocity near the bottom and, since the depth-averaged velocity has to be maintained at 0.5m/s, a slight increase in the upper layers (seen in Figure 4b). For example, calculations suggest that the velocity for stratified case is reduced by 27% (from 14.8cm/s to 10.9cm/s) at bottom to about 1% at 2m above the bed and the difference is less than about 1.2% in the rest portion of the water column.

Since a reduction in shear velocity leads to a smaller reference concentration and stable stratification reduces upward mixing of sediments into the water column, the two effects mentioned above both result in a decrease in suspended sediment concentration. One can therefore expect a significant reduction in the sediment concentration and transport rates due to self-stratification effects. The reference concentrations in Table 1 show that these are reduced by about 7% from 7.23kg/m^3 to 6.75kg/m^3 at $z = 7d$. This very minor reduction is, of course, associated with the virtually unchanged wave shear velocities, which dominate in the creation of the mean reference concentration. Consequently, the concentration within the boundary layer does not show significant reduction as seen in Figure 3b. In contrast, the concentration above the wave boundary layer (shown in Figure 4c) is significantly decreased by the stratification effect, e.g. the concentration at 1m above the bed is reduced by about 68% from 0.28kg/m^3 to 0.09kg/m^3, although the difference between non-stratified and stratified cases is only 13% at bottom.

The transport rates in Table 2 reveal that the net bed-load and mean suspended load transport rates within the boundary layer decrease only by roughly 30%. The relatively small reduction of net bed-load transport rate is because it depends only on the sediment transport shear stress which, as seen from Table 1, does not change appreciably. The reason for the slight reduction of mean suspended load transport rate within the boundary layer reflects primarily the reduction in current velocity (shown in Figure 3a), whereas the concentration (Figure 3b), predicted without considering stratification, hardly changes. However, the suspended load transport rate above the boundary layer is significantly reduced as a result of stratification. The stratified value of 0.12kg/m/s is only 24% of the 0.5kg/m/s predicted when stratification effects are neglected. This significant influence of stratification effects above the boundary layer is mainly caused by the reduction of turbulent mixing associated with the stable stratification and, to a lesser extent, by the reduced current shear stress.

3.3 Effects of Sediment Diameter

In the preceding sections, we discussed wind wave and stratification effects based on numerical results for 0.1mm sediment. To investigate the influence of sediment size on sediment transport, we perform two simulations, one with and the other without stratification effects, for sediment of 0.2mm diameter. The same flow and wave conditions as those for the 0.1mm sediment are used, and results are listed in Tables 1 and 2.

As shown in Table 1, the physical and apparent roughness are about 12cm and 52cm. These are significantly larger than those for the 0.1mm sediment, indicating larger ripples and therefore smaller ratios between skin friction shear velocities and total shear velocities. This is confirmed by the results in Table 1, e.g. the ratio of skin friction and total current shear stress for non-stratified case is 0.26 for 0.2mm sediment compared to 0.46 for 0.1mm sediment. The reference concentrations at $z = 7d$ are quite similar for the 0.1mm and 0.2mm sediments; however, due to its much larger fall velocity, the mean concentration at the outer edge of the bottom boundary layer, 0.75kg/m^{3}for 0.2mm sediment, is only 28% of the value for 0.1mm sediment.

Due to the near-identical critical shear stresses and much different fall velocities for the two sediments, the difference of net bed-load transport rates between the two sediments is smaller than that of suspended load transport rates. As shown in Table 2, the difference of net bed-load transport rates for non-stratified case is about 38%, whereas the difference between suspended transport rates above the boundary layer is as large as 97%.

As for the stratification effect, the results in Table 2 show that the stratification only results in a 12% reduction of total sediment transport rate for 0.2mm sediment, i.e. much less than the 75% reduction found for the 0.1mm sediment. The primary reason for this is that the concentration above the boundary layer is significantly reduced for the 0.2mm sediment due to its much larger fall velocity, 2.2cm/s vs. 0.72cm/s, and therefore generates less stratification effect.

4. CONCLUSIONS

In this paper, a three dimensional sediment transport model is proposed for the computation of sediment transport in combined wave-current flows in coastal waters. The model calculates three contributions to the total sediment transport rate: (i) net bed-load transport in the bed-load layer $z < 7d$; (ii) mean suspended load transport within the bottom boundary layer $7d < z < \delta_{cw}$; and (iii) suspended load transport above the wave boundary layer $z > \delta_{cw}$. Wind wave effects on flow and sediment transport are accounted for through an analytical bottom boundary layer model. For the hydrodynamics, the presence of wind waves enhances the flow resistance by increasing the roughness, the so-called apparent roughness, experienced by a current in the presence of waves. For the sediment transport processes, wind waves increase the bottom shear stress and the near-bed turbulence and therefore mobilize and suspend more sediment than would be the case if the waves were absent. In addition, the wave enhanced turbulent mixing in the water column above the wave boundary layer diffuse more sediment up into the water column. In the water column above the wave boundary layer hydrodynamics and sediment transport processes are solved numerically using POM and stratification effects induced by suspended sediment are taken into account. Idealized tests were performed to examine the model's ability to predict sediment transport in combined wave-current flows.

The test results reveal that wind waves have a pronounced effect on hydrodynamics and suspended sediment transport for typical conditions of coastal waters, e.g. sediment may only be mobilized and transported when wind waves are present. The sediment transport rate within the wave boundary layer, which has been neglected in most previous studies, is more important for coarser sediment, e.g. it is about 20% the suspended load transport above the boundary layer for 0.2mm sediment compared to 1% for 0.1mm sediment case in the present study's computational example. Therefore, wind wave effects should never to be neglected in sediment transport modeling in coastal waters.

The numerical tests suggest that the self-stratification effect is more significant for fine sediment as it causes 75% drop in total transport rate for the 0.1mm sediment case, but becomes less significant for coarser sediment as the reduction of total transport rate is only 12% for 0.2mm sediment. Essentially, the stratification effect can be very significant when concentration gradients are large, which usually happens for relatively fine sediment and strong flow conditions. In such circumstances, our results show that the self-stratification effect should be accounted for when modeling sediment transport in coastal waters.

It is noted that the present model tests were performed for a steady co-directional wave-current flow. Further tests must be conducted to test the model's capabilities in more realistic flows, e.g. in unsteady flows and in the cases where waves and current are in different directions. For unsteady, slowly varying flows, the applicability of the concentration bottom boundary condition, which assumes equilibrium conditions, needs to be tested. To more accurately predict the sediment transport in combined wave-current flows, the wave-associated suspended load transport within the wave boundary layer, $\tilde{q}_{S1} = \int_{7d}^{\delta_{cw}} \tilde{u}\tilde{C}dz$, with $\tilde{u}(t)$ and $\tilde{C}(t)$ denoting the time-varying wave-associated velocity and concentration within the wave boundary layer, should be included. Considering the significant influence of self-stratification on suspended transport above the boundary layer, it would be prudent to examine the effect of stratification within the wave boundary layer, or in the extrapolation of the mean concentration from the outer edge of the wave boundary layer to the numerical model's grid point where a reference concentration is specified. We are currently pursuing extensions of the sediment transport model along these lines as well as examining its performance in more realistic scenarios.

ACKNOWLEDGMENTS

The research described in this paper was funded in whole or in part by the Singapore National Research Foundation (NRF) through the Singapore-MIT Alliance for Research and Technology's (SMART) Center for Environmental Sensing and Modeling (CENSAM).

REFERENCES

Blumberg, A.F., B. Galperin, and D.J. O'Connor. 1992. Modeling vertical structure of open-channel flows, *Journal of Hydraulic Engineering*, 118(H8), 1119-1134.

Blumberg, A.F., and G.L. Mellor. 1987. A description of a three-dimensional coastal ocean circulation model, Three Dimensional Coastal Ocean Models, *N. Heaps, Ed., Coastal Estuarine Science*, Vol. 4, Amer. Geophys. Union, 1–16.

Grant, W.D., and O.S. Madsen. 1979. Combined wave and current interaction with a rough bottom, *Journal of Geophysical Research*, 84(C4), 1797-1808.

Herrmann, M.J., and O.S. Madsen. 2007. Effect of stratification due to suspended sand on velocity and concentration distribution in unidirectional flows, *Journal of Geophysical Research*, 112, C02006, doi:10. 1029/2006JC003569.

Humbyrd, C.J., and O.S. Madsen. 2010. Predicting movable bed roughness in coastal waters, *Proceedings of the International Conference on Coastal Engineering*. *No. 32(2010),* Shanghai, China. Paper #: sediment.6. Retrievable from http://journals.tdl.org/ICCE/

Jiménez, J.A. and O.S. Madsen. 2003. A simple formula to estimate settling velocity of natural sediment, *Journal of waterway, port, coastal and ocean engineering*, 129, No.2, 70-78.

Lesser, G.R., J.A. Roelvink, J.A.T.M. van Kester, and G.S. Stelling. 2004. Development and validation of a three-dimensional morphological model, *Coastal Engineering*, 51, 883-915.

Li, M.Z. and C.L. Amos. 2001. SEDTRANS96: the upgraded and better calibrated sediment-transport model for continental shelves, *Computers & Geosciences*, 27(6), 619-645.

Madsen, O.S. (1991) Mechanics of cohesionless sediment transport in coastal waters. *Proceedings of Coastal Sediments '91*, ASCE, Seattle, USA. 1:15-27

Madsen, O.S. 1994. Spectral wave-current bottom boundary layer flows. *Proceedings of 24th International Conference on Coastal Engineering*, ASCE, 384-398.

Madsen, O.S. 2002. Sediment Transport Outside the Surf Zone. In: Walton, T. (editor), *Coastal Engineering Manual, Part III, Coastal Processes, Chapter III-6, Engineer Manual* 1110-2-1100, U.S. Army Corps of Engineers, Washington, DC.

Mellor, G.L., and T. Yamada. 1982. Development of a turbulence closure model for geophysical fluid problems, *Review of Geophysics and Space Physics*, 20, 851–875.

Warner, J.C., C.R. Sherwood, H.G. Arango, and R.P. Signell. 2005. Performance of four turbulence closure models implemented using a generic length scale method, *Ocean Modelling*, 8, 81-113.

Warner, J.C., C.R. Sherwood, R.P. Signell, C.K. Harris, and H.G. Arango. 2008. Development of a three-dimensional, regional, coupled wave, current and sediment-transport model, *Computers & Geosciences*, 34, 1284-1306.